Macromolecules **1989**, *22*, 617–622

(42) Masin, F.; Gusman, G.; Deltour, R. *Solid State Commun.* **1981**, *39*, 505.
(43) Ziliox, M.; Francois, B.; Mathis, C.; Meurer, B.; Spegt, P.; Weill, G. *J. Phys. Chem. Solids* **1983**, *44*, C3-361.
(44) Nechtschein, M.; Devreux, F.; Greene, R. L.; Clarke, T. C.; Street, G. B. *Phys. Rev. Lett.* **1980**, *44*, 356.
(45) Maresch, G. G.; Kendrick, R. D.; Yannoni, C. S.; Galvin, M. E. *Macromolecules*, in press.
(46) Mehring, M.; Seidel, H.; Muller, W.; Wegner, G. *Solid State Commun.* **1983**, *45*, 1075.
(47) Holczer, K.; Roucher, J. P.; Devreux, F.; Nechtschein, M. *Phys. Rev. B.: Condens. Matter* **1981**, *23*, 1051.
(48) Greenbaum, S. G.; Mattix, L.; Resing, H. A.; Weber, D. C. *Phys. Lett. A* **1983**, *98A*, 299.
(49) Ito, T.; Shirakawa, H.; Ikeda, S. *J. Polym. Sci., Polym. Chem. Ed.* **1974**, *12*, 11.
(50) Galvin, M. E.; Wnek, G. E. *Polym. Commun.* **1982**, *23*, 795.
(51) Galvin, M. E.; Wnek, G. E. *J. Polym. Sci., Polym. Chem. Ed.* **1983**, *21*, 2727.
(52) Galvin, M. E. Ph.D. Thesis, Massachusetts Institute of Technology, 1984.
(53) Jelinski, L. W.; Dumais, J. J.; Engel, A. K. *Macromolecules* **1983**, *16*, 492.
(54) Davis, J. H.; Jeffrey, K. R.; Bloom, M.; Valic, M. I.; Higgs, T. P. *Chem.* Phys. *Lett.* **1976**, *42*, 390.
(55) Blinc, R.; Rutar, V.; Seliger, J.; Slak, J.; Smolej, V. *Chem. Phys. Lett.* **1977**, *48*, 576.
(56) Hentschel, R.; Spiess, H. W. *J. Magn. Reson.* **1979**, *35*, 157.
(57) Mehring, M. *High Resolution NMR in Solids*, 2nd ed.; Springer-Verlag: New York, 1983.
(58) Bloom, M.; Davis, J. H.; Valic, M. I. *Can. J. Phys.* **1980**, *58*, 1510.
(59) Dumais, J. J.; Cholli, A. L.; Jelinski, L. W.; Hedrick, J. L.; McGrath, J. E. *Macromolecules* **1986**, *19*, 1884.
(60) Messager, J. C.; Sanquer, M.; Baudour, J. L.; Meinnel, J. Proceedings, First European Crystallography Meeting Bordeaux, France, 1973.
(61) Baudour, J. L.; Delugeard, Y.; Sanquer, M. *Acta Crystallogr.* **1974**, *B30*, 691.
(62) Delugeard, Y.; Desuche, J.; Baudour, J. L. *Acta Crystallogr.* **1976**, *B32*, 702.
(63) Kovacic, P.; Feldman, M. D.; Kovacic, J. P.; Lando, J. B. *J. Appl. Polym. Sci.* **1968**, *12*, 1735.
(64) Froyer, G.; Maurice, F.; Mercier, J. P.; Rivière, D.; LeCun, M.; Auvray, P. *Polymer* **1981**, *22*, 1981.
(65) Baughman, R. H.; Brèdas, J. L.; Chance, R. R.; Elsenbaumer, R. L.; Shacklette, L. W. *Chem. Rev.* **1982**, *82*, 209.
(66) Murray, D. P.; Dechter, J. J.; Kispert, L. D., *J. Polym. Sci., Polym. Lett. Ed.* **1984**, *22*, 519.
(67) Jelinski, L. W.; Melchior, M. T. In *Practical NMR Spectroscopy*; Dybowski, C., Lichter, R., Eds.; Marcel Dekker: New York, 1986.
(68) VanderHart, D. L.; Earl, W. L.; Garroway, A. N. *J. Magn. Reson.* **1981**, *44*, 361.
(69) Gullion, T.; Conradi, M. S. *Phys. Rev. B.: Condens. Matter* **1984**, *30*, 1133.
(70) Jelinski, L. W., unpublished data.
(71) Hentschel, D.; Sillescu, H.; Spiess, H. W. *Macromolecules* **1981**, *14*, 1605.
(72) Galvin, M. E.; Higgins, J., unpublished data.

Analysis of the Surface Structure of a Built-Up Film of Fluorocarbon Amphiphile and Polymer/(Fluorocarbon Amphiphile) Composite Thin Film by Means of X-ray Photoelectron Spectroscopy

Atsushi Takahara, Naoaki Morotomi, Shoji Hiraoka, Nobuyuki Higashi,[†] Toyoki Kunitake,[‡] and Tisato Kajiyama[*]

Departments of Applied Chemistry and Organic Synthesis, Faculty of Engineering, Kyushu University 36, Hakozaki, Higashi-ku, Fukuoka 812, Japan.

Received February 16, 1988

ABSTRACT: Angular dependent X-ray photoelectron spectra were obtained for the Langmuir–Blodgett (LB or built-up) film of a fluorocarbon amphiphile with two fluoroalkyl chains and a poly(vinyl alcohol)/(fluorocarbon amphiphile) composite thin film. A simple layer model was proposed to estimate the photoelectron mean free path in fluorocarbon bilayers. A comparison of the angular dependences of the observed XPS intensity with the calculated intensity for built-up film revealed that the photoelectron mean free path for C_{1s} photoelectron (kinetic energy of ca. 970 eV) in built-up film is ca. 4.0 nm. Fluorocarbon amphiphilic molecules in the composite thin film form highly oriented bilayer lamella. The surface enrichment of fluorocarbon amphiphile in the surface of the composite thin film facing the air was confirmed by X-ray photoelectron spectroscopy. Application of layer models to the calculation of the composition profile of the composite thin film revealed that the surface of the composite thin film which contains more than 19 wt % amphiphile was completely covered with an oriented bilayer of the amphiphile.

Introduction

The structure and properties of Langmuir–Blodgett (LB or built-up) films have received much attention recently. This is due to the fact that the control of the state of molecular aggregation is easily achieved by the preparation technique developed by Langmuir[1] and Blodgett.[2] Application studies concerning electron conduction, semiconductors, biomaterials, etc. have been carried out by several authors.[3-5]

X-ray photoelectron spectroscopy is a useful technique to characterize the surface composition of solids. Estimation of the photoelectron mean free path in organic solids has been achieved by utilizing built-up films.[6-8] Since the built-up film forms a highly ordered layer structure, it is a suitable material for the estimation of the photoelectron mean free path. The electron mean free path of the C_{1s} photoelectron (kinetic energy of ca. 970 eV) in the built-up films of long-chain fatty acids ranges from 4 to 5 nm.[8]

A series of amphiphiles containing fluoroalkyl chains have been synthesized by Kunitake and co-workers.[9,10] Fluorocarbon amphiphiles form a bilayer structure in water and show phase transition behavior similar to that observed for biological lipids or artificial hydrocarbon amphiphiles.[11-13] The fluorocarbon amphiphiles can be immobilized by casting an aqueous solution of amphiphile with aqueous poly(vinyl alcohol).[14] The fluorocarbon amphiphile molecules in this composite thin film form highly

---

[*] Author to whom correspondence should be addressed.

[†] Present address: Department of Applied Chemistry, Faculty of Engineering, Doshisha University, Karasuma Imadegawa, Kamigyo-ku, Kyoto 602, Japan.

[‡] Department of Organic Synthesis.

0024-9297/89/2222-0617$01.50/0

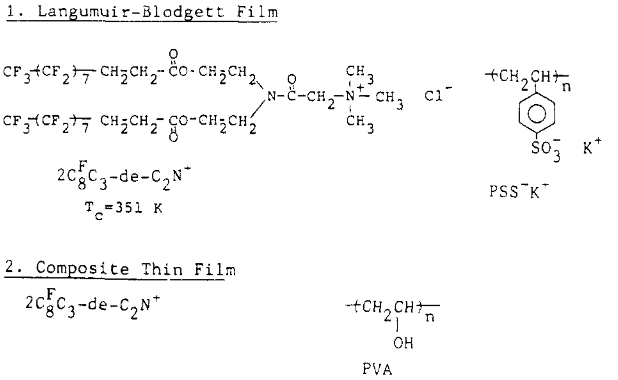

Figure 1. Chemical structures of fluorocarbon amphiphile and polymers used for the preparation of the built-up film and the composite thin film.

oriented lamellae similar to those of built-up film.[15-17]

In this study, the Langmuir–Blodgett (built-up) film of a fluorocarbon amphiphile with two fluoroalkyl chains was prepared and the angular dependent X-ray photoelectron spectra were measured in order to estimate the photoelectron mean free path. Also, a composite thin film of the fluorocarbon amphiphile and poly(vinyl alcohol) was prepared, and its surface structure was analyzed on the basis of the overlayer model.

Experimental Section

1. **Preparation of Built-Up Film.** Figure 1 shows the chemical structures of the fluorocarbon amphiphile and polymers used for the preparation of LB film and the composite thin film. The preparation of this amphiphile has been described elsewhere.[9,10] The surface pressure (π)–area (A) isotherms were obtained in order to determine the preparation conditions for the built-up film. The amphiphile was dissolved in an ethanol–benzene mixture (1:9 vol ratio) and spread on an aqueous solution of potassium poly(styrenesulfonate) (PSS$^-$K$^+$, 2×10^{-5} unit mol/L in monomer unit) at 293 K. The measurement of the surface pressure (π)–area (A) curves and the deposition of surface monolayer were conducted by using a microprocessor-controlled film balance (FSD-20, San-Esu Keisoku Co., Ltd.)

2. **Preparation of Composite Thin Film.** The fluorocarbon amphiphile and poly(vinyl alcohol) were used for the preparation of the composite thin films. The fluorocarbon amphiphile forms a stable bilayer membrane in water, which was dispersed in water by sonication. The dispersion was mixed with a water solution of poly(vinyl alcohol) (PVA) (MW = 154 000). The composite thin film was prepared by casting a water solution of PVA with amphiphile on a clean glass plate at room temperature. The weight percentages of the amphiphile in the composite thin film were 19, 38, 58, and 83.

3. **Sample Characterization.** Wide-angle X-ray diffraction (WAXD) and small-angle X-ray scattering (SAXS) patterns of the built-up film and the composite thin films were obtained by means of a photographic method. Cu Kα X-ray beams were generated with a Rigaku X-ray generator RU-200.

4. **X-ray Photoelectron Spectroscopy.** The X-ray photoelectron spectra of the built-up films and the composite thin film were obtained with a Shimadzu ESCA750. The X-ray source was Mg Kα, which was obtained at 8 kV and 30 mA. The samples were attached to the probe, which was cooled to 233–243 K to avoid degradation and evaporation of the amphiphilic molecules during XPS measurement. Spectra were obtained in digital form. Curve fitting of the spectra was achieved by using a nonlinear least squares method to fit the digital data. The program used is SALS.[18] A Gaussian–Lorentzian product function was assumed for the curve-fitting process.

Results and Discussion

1. **Transfer Behavior of Monolayer.** Figure 2 shows the surface pressure (π)–area (A) isotherms for the monolayer of fluorocarbon amphiphile at the subphase temperature of 293 K. The subphase was pure water (broken line) and an aqueous solution of PSS$^-$K$^+$ (solid line). The π–A isotherms for the amphiphile show a solid condensed phase above a surface pressure of ca. 30 mN m^{-1}. Extrapolation of the linear portion of the condensed phase to zero pressure gave molecular areas of ca. 0.50 nm^2. This value is twice as big as the molecular cross section of the fluorocarbon chain. The monolayer on the PSS$^-$K$^+$ subphase shows the condensed phase occurs at a lower surface pressure than on a pure water subphase. This is due to polyion complex formation between the ammonium group in the amphiphile and the sulfonate group in PSS. Multilayers of the fluorocarbon amphiphile–PSS complex were built up on the polystyrene substrate by the Langmuir–Blodgett method. The buildup on the substrate was carried out at a surface pressure of 35 mN m^{-1}. Figure 3 is a histogram showing the apparent transfer ratio for the monolayer of fluorocarbon amphiphile with PSS$^-$K$^+$ subphase onto the polystyrene substrate. The monolayer on a pure water surface could not be deposited at 293 K under a surface pressure of 35 mN m^{-1}. For the monolayer on PSS$^-$K$^+$ subphase, the transfer ratio during the down and up strokes was almost unity. This indicates that an almost Y-type membrane was obtained.

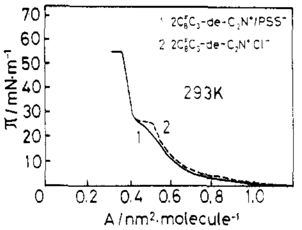

Figure 2. Surface pressure (π)–area (A) isotherms for a monolayer of fluorocarbon amphiphile at 293 K on pure water (broken line) and aqueous solution potassium poly(styrenesulfonate) (solid line) subphase.

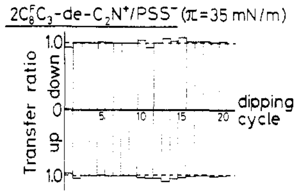

Figure 3. Transfer behavior of monolayer of fluorocarbon amphiphile with aqueous solution of potassium poly(styrenesulfonate) subphase on polystyrene substrate.

2. **Structure of Built-Up Film and Composite Thin Film.** The structure of built-up film was analyzed by means of wide-angle X-ray diffraction (WAXD) and small-angle X-ray scattering (SAXS). Figure 4 shows the wide-angle X-ray diffraction and small-angle X-ray scattering patterns of the fluorocarbon amphiphile–PSS built-up film. The X-ray beams were directed parallel to the film surface, as shown in Figure 4. The highly oriented diffractions of 4.40, 2.32, 1.55, and 1.15 nm were observed on the equator of the small angle region. Since the reciprocal ratio of these spacings is 1:2:3:4..., it is assumed that the fluorocarbon amphiphilic molecules in the built-up film will form bimolecular lamella.[19] The long period for the built-up film was 4.4 nm, which agrees fairly well with the period obtained from the WAXD pattern of crystalline fluorocarbon amphiphile powder.[17] These results indicate that the built-up film is formed as a Y-type membrane, this being expected from the transfer behavior shown in Figure 3. Since the bimolecular length of this amphiphile, evaluated from a CPK molecular model, is 4.9 nm, it is supposed that the amphiphile molecule may tilt ca. 30° perpendicular to the film surface. However, the off-meridional spots corresponding to the intermolecular distance

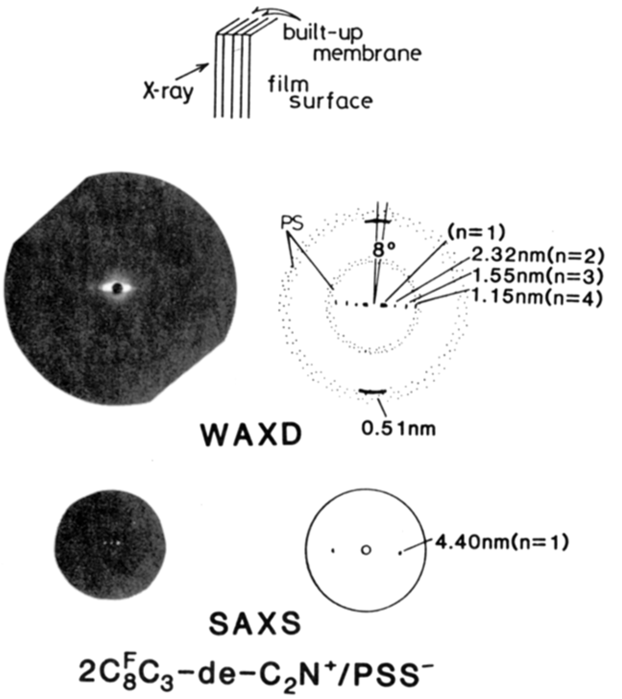

Figure 4. Wide-angle X-ray diffraction and small-angle X-ray scattering patterns for the built-up film of fluorocarbon amphiphile prepared through polyion–complex formation.

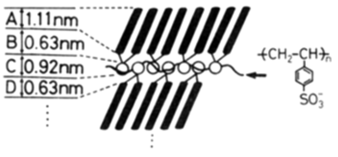

Figure 5. Schematic representation of the structure model of a bilayer of fluorocarbon amphiphile–PSS polyion complex.

suggest that each molecule tilts ca. 8° to the normal. Thus the structure in Figure 5 is proposed. In this model, each fluorocarbon chain tilts 8° to the normal, and mutual insertion of hydrophilic sections is assumed. Since the cross section of the hydrophobic fluorocarbon part is larger than that of the hydrophilic part, it is reasonable to assume a mutual insertion of hydrophilic groups. The highly ordered structure of this built-up film is appropriate as a model material for XPS measurement.

The state of aggregation of the amphiphilic molecules in the composite thin film was studied by wide-angle X-ray diffraction. Figure 6 shows the wide-angle X-ray diffraction patterns of the composite thin films containing 19 and 83 wt % of fluorocarbon amphiphiles. When the X-ray beam was directed perpendicular to the film surface (TV), two Debye rings corresponding to the intermolecular spacings of 0.46 and 0.49 nm were observed. When the X-ray beam was irradiated parallel to the film surface (EV), the WAXD showed the orientation of fluorocarbon amphiphilic molecules perpendicular to the film surface. The reflections observed on the meridian are 4.33, 2.16, 1.46, 1.07, 0.72 ... nm. Since the reciprocal ratio of these reflection is 1:2:3:4:..., it is concluded that the fluorocarbon amphiphile in the composite membrane forms bimolecular lamella. The formation of this oriented lamella was observed for the composite membrane having 19 wt % fluorocarbon amphiphile. The intensity corresponding to the fluorocarbon amphiphile became more distinct with an increase in the weight fraction of fluorocarbon amphiphile.

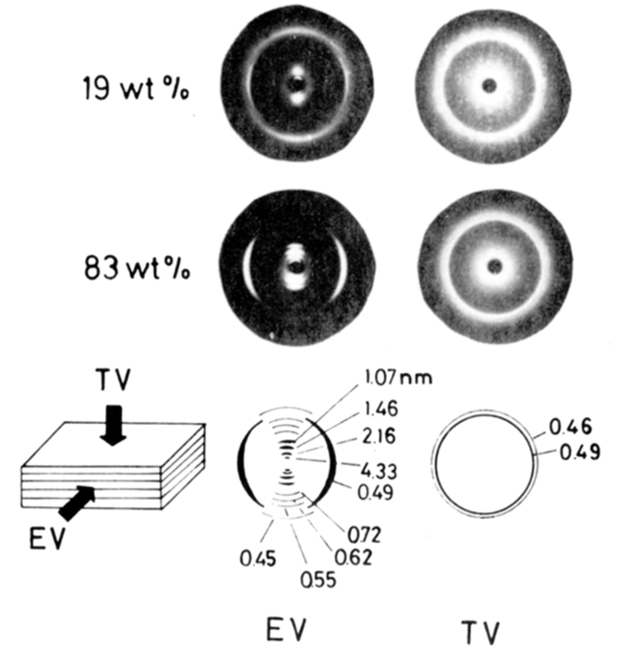

Figure 6. Wide-angle X-ray diffraction patterns for the composite thin film containing 19 and 83 wt % of fluorocarbon amphiphile. TV and EV denote through view and edge view, respectively.

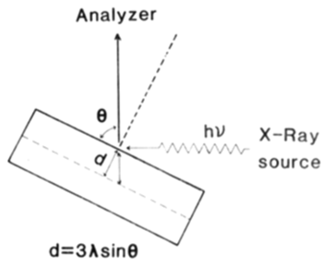

Figure 7. Schematic representation of the relationship between the incident X-ray beam and an emitted photoelectron.

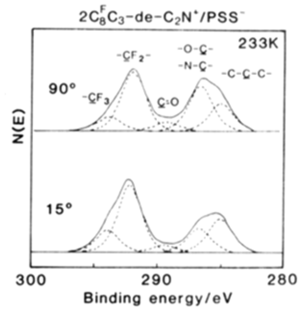

Figure 8. Angular dependent C_{1s} spectra for the Langmuir–Blodgett (built-up) film of fluorocarbon amphiphile–PSS polyion complex at 233 K.

3. Evaluation of Photoelectron Mean Free Path in Built-Up Film of Fluorocarbon Amphiphile–PSS Polyion Complex. Figure 7 shows the relationships between the incident X-ray beam and the emitted photoelectron, where θ, λ, and d are the take-off angle of the emitted photoelectron, the photoelectron mean free path, and the sampling depth, respectively. The sampling depth, d, is proportional to the mean free path and sin θ.[20] Therefore, the signal from the surface region increases with a decrease in the take-off angle.

Figure 8 is the C_{1s} spectra of the built-up film of fluorocarbon amphiphile–PSS polyion complex obtained for the take-off angles of 90° and 15°. The XPS measurement was carried out at a specimen temperature of 233 K at which degradation of amphiphile was not observed. The C_{1s} peak corresponding to the neutral aliphatic and aromatic carbons is observed at 285.0 eV. The C_{1s} peak ob-

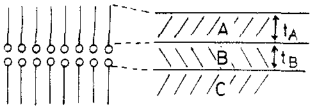

Figure 9. Overlayer model for the evaluation of electron mean free path in the built-up film of fluorocarbon amphiphile–PSS polyion complex.

served at 286.6 eV is assigned to the carbon adjacent to nitrogen and ether oxygen. The C_{1s} peak corresponding to the carbonyl carbon is observed at 288.6 eV. Also, the peaks at 292.1 and 294.4 eV were assigned to the C_{1s} peaks from CF_2 and CF_3, respectively. The relative intensity of fluorocarbon to the total C_{1s} intensity increased with a decrease in the take-off angle. This is due to the fact that the hydrophobic fluorocarbon group exists on the interface region between air and built-up film. The location of each carbon in the built-up film can be determined from the results of the wide-angle X-ray diffraction. Also, the specimen shows the S_{2p} peak at ca. 169 eV which is assigned to the sulfonate group of PSS.

Since sulfur atoms in PSS exist at the hydrophilic group in the built-up film, the magnitude of the electron mean free path in the built-up film can be evaluated from the variation of the relative intensity ratio of S_{2p} to C_{1s} with the take-off angle. This is done by comparing the measured intensity with calculated intensity based on the location of carbon atoms determined from WAXD. It is possible to obtain the experimental intensity ratio of sulfur to carbon atoms by correcting for the kinetic energy dependence and photoionization cross section.[20] Thus, the number ratio of sulfur to carbon atoms was evaluated from a simple layer model.[8,21,22] Figure 9 shows the layer model for the built-up film of amphiphile. Since the atomic concentration distribution can be defined from this layer model, the variation of the XPS intensity with the take-off angle can be calculated from the following equations:

$$I_A \propto N_A(1 - \exp(-t_A/\lambda_C \sin\theta)) \qquad (1)$$

$$I_B \propto KN_B(1 - \exp(-t_B/\lambda_S \sin\theta))\exp(-t_A/\lambda_S \sin\theta) \qquad (2)$$

$$I_C \propto N_C \exp(-t_B/\lambda_C \sin\theta)\exp(-t_A/\lambda_C \sin\theta) \qquad (3)$$

where A, B, and C are the carbon atoms in the outermost surface, the sulfur atoms in hydrophilic group, and the carbon atoms in the second layer, respectively. N_A, N_B, and N_C are the concentrations of each atom in each phase. K in eq 2 is the correction factor including the difference in photoelectron ionization cross section and kinetic energy between sulfur and carbon atoms. λ_C and λ_S are photoelectron mean free paths for carbon and sulfur atoms. It is assumed that the dependence of λ on the kinetic energy of a photoelectron follows Ashley's equation.[23,24] t_A and t_B are the thickness of each layer obtained from wide-angle X-ray diffraction. The relative intensity ratio of sulfur to carbon atoms can be calculated from

$$X = I_B/I_{\text{carbon}} \qquad (4)$$

where I_{carbon} is the total intensity of C_{1s}. This calculation was carried out by extending this equation up to the seventh layer. It is verified that the contribution of the deeper layer can be neglected.

Figure 10 shows a plot of the angular dependence of the relative intensity ratio of S_{2p} to C_{1s} (S/C) for the built-up film, which is normalized by the S/C at a take-off angle of 90°. The calculated value of S/C was obtained on the basis of the value of the layer model shown in Figure 9. The experimental data (open circles) agree with the calculated intensity curve if the mean free path for C_{1s} electrons is assumed to be 3–4 nm. This value is quite similar to that obtained from the Ashley parameters.[23,24]

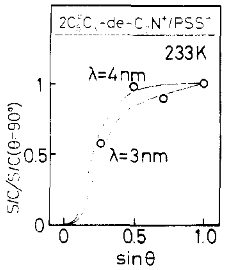

Figure 10. Variation of the relative intensity ratio of the number of sulfur to carbon atoms (S/C) for the built-up film of fluorocarbon amphiphile–PSS polyion complex with the take-off angle of the photoelectron. (○, observed; —, calculated).

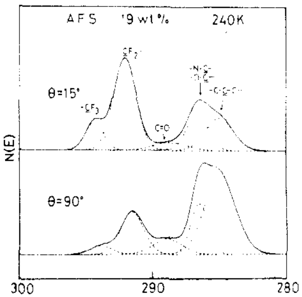

Figure 11. C_{1s} spectra for the air-facing surface (AFS) of the composite thin film containing 19 wt % fluorocarbon amphiphile at the take-off angles of 15° and 90°.

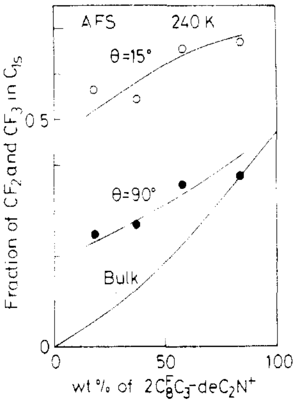

Figure 12. Variation of the fraction of fluorocarbon in total C_{1s} on the AFS of the composite thin film with weight percent of fluorocarbon amphiphile at the take-off angles of 15° and 90°.

4. Surface Composition Profile of Composite Thin Film. The surface structure of the composite thin film was evaluated by means of XPS. Figure 11 shows the XPS spectra of C_{1s} for the air-facing surface (AFS) of the composite thin film containing 19 wt % fluorocarbon amphiphile at the take-off angles of 90° and 15°. The C_{1s} peak observed at 286.3 eV is mainly contributed by the ether carbon in PVA. However, the C_{1s} peaks at 292.1 and 294.4 eV are assigned to the fluorocarbon groups. Thus, the relative intensity of C_{1s} from fluorocarbon to the total C_{1s} corresponds to the fraction of fluorocarbon on the surface. The relative intensity of fluorocarbon to the total C_{1s} for a take-off angle of 15° was greater than that for a take-off angle of 90°. The analytical depth in the case of the take-off angle of 15° is one-fourth that of a take-off angle of 90°. This indicates that the concentration of fluorocarbon on an outermost is larger than that of an inner one.

Figure 12 shows the variation of the fraction of fluorocarbon in the total C_{1s} for AFS of the composite thin film with the weight fraction of fluorocarbon amphiphile. The

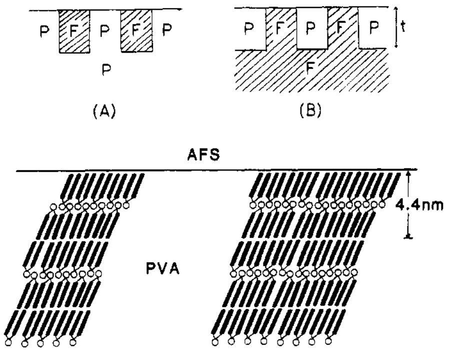

Figure 13. Overlayer model for composite thin film. F and P are the bimolecular lamella of fluorocarbon amphiphile and the poly(vinyl alcohol) layer, respectively.

"bulk" indicates the fraction of fluorocarbon in total carbon calculated from the elemental composition of each specimen. For a take-off angle of 90°, the relative intensity of fluorocarbon increased with the fraction of fluorocarbon amphiphile in bulk. The relative intensity of fluorocarbon in the lower fraction region of fluorocarbon amphiphile was larger than the calculated "bulk" value. This is due to the enrichment of fluorocarbon amphiphile on AFS. This occurs because of the extremely low surface free energy of the fluorocarbon groups in the amphiphile. With an increase in the weight fraction of amphiphile, the relative intensity of fluorocarbon for the take-off angle of 90° approaches the bulk value. The relative intensity of fluorocarbon for the take-off angle of 15° is larger than that of 100% fluorocarbon amphiphile. This may be ascribed to the orientation of fluorocarbon chains to the interface between air and the composite thin film.

For the quantitative analysis, a simple layer model[25] was applied to the analysis of the surface composition of this composite thin film. Figure 13 shows the patchy overlayer model for the composite thin film; P and F denote poly(vinyl alcohol) (PVA) and bimolecular membrane of fluorocarbon amphiphile, respectively. t in Figure 13 corresponds to the layer thickness of fluorocarbon amphiphile in the composite thin film. Since the fluorocarbon amphiphiles form bimolecular lamella, t is a multiple of bilayer thickness 4.4 nm. For simplicity, it is assumed that the concentration of each atom functional group is constant in each layer. If we assign N_F, N_B, and N_P as the atomic percent of fluorocarbon in the F layer, of carbon atoms except fluorocarbon in the F layer, and of total carbon in the P layer, the contribution of each carbon atom to the C_{1s} peak is expressed by

$$I_F \propto N_F G(1 - \exp(-t/\lambda_C \sin \theta)) \quad (5)$$

$$I_B \propto N_B G(1 - \exp(-t/\lambda_C \sin \theta)) \quad (6)$$

$$I_P \propto N_P(1 - G + G \exp(-t/\lambda_C \sin \theta)) \quad (7)$$

where I_F, I_B, and I_P are the intensities from fluorocarbon in the F layer, from carbon atoms except for fluorocarbon in the F layer, and from total carbon in the P layer. G is a variable which indicates the fraction of the surface area covered with bimolecular lamella of fluorocarbon amphiphile. The magnitude of λ_C employed was 4 nm and was obtained for built-up film of fluorocarbon amphiphile. The fraction of fluorocarbon in the total C_{1s} is expressed as

$$X_F = I_F/(I_F + I_B + I_P) \quad (8)$$

The actual calculation was carried out by expanding the model up to the seventh layer. Another calculation was carried out for the layer model in which PVA layers exist as an overlayer of bimolecular lamella of fluorocarbon amphiphile (Figure 13b). Since the fluorocarbon group shows low surface free energy compared with that of PVA, the model with fluorocarbon bilayer as an overlayer (Figure 13a) has been employed.

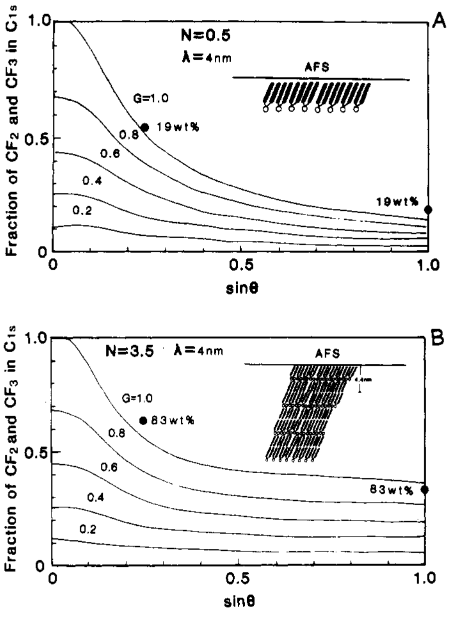

Figure 14. Variation of calculated fraction of fluorocarbon in total C_{1s} for the AFS of the composite thin film with take-off angle as a function of the surface coverage ratio, G, based on the patchy overlayer model. The number of bilayers on the outermost surface is 0.5 (A) and 3.5 (B), respectively. Closed circles indicate the observed fraction of fluorocarbon for the composite thin film.

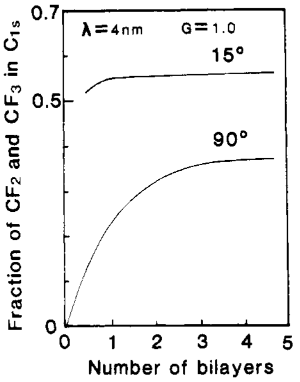

Figure 15. Variation of calculated fraction of fluorocarbon in total C_{1s} with the number of bilayers on the outermost surface at the take-off angles of 15° and 90°.

Figure 14 shows the variation of the fraction of fluorocarbon in total C_{1s} with the take-off angle of the photoelectron as a function of the fraction of surface coverage G with bilayer lamella of fluorocarbon amphiphile. The number of continuous bilayers on the outermost layer in Figure 14 is 0.5 (A) and 3.5 (B). The calculated curve in the case that the surface is completely covered with a bimolecular lamella of fluorocarbon amphiphile for the take-off angles of 15° and 90° agreed fairly well with the observed value for the composite thin film with 19 wt % of fluorocarbon amphiphile. This indicates that even for a small bulk fraction of amphiphile surface coverage with fluorocarbon amphiphile occurs due to the small surface free energy of the fluoroalkyl group. The calculated curve for complete coverage with more than four continuous layers agreed fairly well with the observed value for the composite thin film with 83 wt % fluorocarbon amphiphile. Figure 15 exhibits the variation of the fraction of fluorocarbon to the total carbon with the number of bilayers at the outermost surface in the case of complete surface

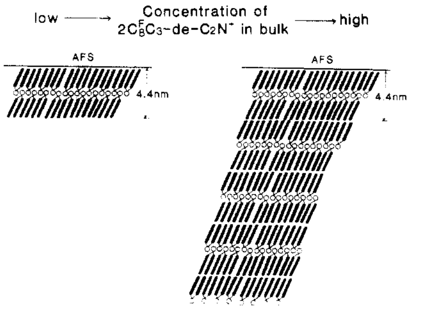

Figure 16. Schematic representation of the structure of the outermost layer of the composite thin film with small and large weight percents of fluorocarbon amphiphile.

Table I
Number of Bilayers on the Surface of the Polymer/Fluorocarbon Amphiphile Composite Thin Film

wt % amphiphile	no. of bilayers	wt % amphiphile	no. of bilayers
19	0.9	58	3.8
38	1.5	83	>4.0

coverage with fluorocarbon amphiphile bilayer. The comparison between the observed fraction and the calculated one at the take-off angles of 15° and 90° gives the number of repeating bilayers on the surface. Table I summarizes the apparent magnitude of the number of bilayers on the surface of the composite thin film. Since PVA is a hydrophilic polymer, the fluorocarbon amphiphiles orient the hydrophilic group to PVA at their interfacial parts between PVA and amphiphile.

The surface molecular aggregation structure of the composite thin film is schematically represented in Figure 16. In the case of the composite thin film with a small fraction of amphiphile, the whole film surface is completely covered with monolayer or bimolecular lamella of amphiphilic molecules. With an increase in fraction of fluorocarbon amphiphile in composite thin film, the thickness of the bilayer which orients its fluoroalkyl group to the air increased with the fraction of fluorocarbon amphiphile in the bulk. The surface of the composite thin film with 83 wt % fluorocarbon amphiphile is completely covered with continuous bilayers. It has been reported that permselectivity of oxygen to nitrogen gases, α, of this composite thin film showed a large magnitude even if the fraction of fluorocarbon amphiphile was very small.[14] This surface structure analysis revealed that this increase in α is due to the enrichment of fluorocarbon amphiphile on the outermost surface of the composite thin film.

Conclusion

The surface chemical analysis of the Langmuir–Blodgett (built-up) film of fluorocarbon amphiphile and the fluorocarbon amphiphile/poly(vinyl alcohol) composite thin film was carried out by means of X-ray photoelectron spectroscopy. A simple layer model was proposed in order to estimate angular dependence of X-ray photoelectron spectra. The comparison of the observed intensity with the calculated intensity for the built-up film based on a layer model revealed that the photoelectron mean free path for C_{1s} photoelectron (kinetic energy of ca. 970 eV) in the built-up film is 3–4 nm. The WAXD measurement revealed that the fluorocarbon amphiphile in the composite thin film formed highly oriented bimolecular lamellae. The surface enrichment of fluorocarbon amphiphile on the surface of the composite thin film was confirmed by X-ray photoelectron spectroscopy. A layer model was applied to the composite thin film in order to investigate the state of molecular aggregation in the composite thin film. It was concluded that the surface of the composite thin film was completely covered with oriented fluorocarbon amphiphile lamella even when the fraction of amphiphile was 19 wt %.

Registry No. PVA, 9002-89-5; PSS^-K^+, 26949-28-0; $(F_3C(CF_2)_7CH_2CH_2CO_2(CH_2)_2)_2NCOCH_2N^+(CH_3)_3Cl^-$, 116997-55-8.

References and Notes

(1) Langmuir, I. *J. Am. Chem. Soc.* **1917**, *39*, 1848.
(2) Blodgett, K. *J. Am. Chem. Soc.* **1935**, *57*, 1007.
(3) *Thin Solid Films* **1986**, 132–134.
(4) Oda, T.; Takahara, A.; Uchida, M.; Kajiyama, T. *Nippon Kagaku Kaishi* **1987**, 2163.
(5) Sugi, M. *Thin Solid Films* **1987**, *152*, 305.
(6) Larsson, K.; Nordling, C.; Siegbahn, K.; Stenhagen, E. *Acta Chem. Scand.* **1966**, *20*, 2880.
(7) Hall, S. M.; Andrade, J. D.; Ma, S. M.; King, R. N. *J. Electron. Spectrosc. Relat. Phenom.* **1979**, *17*, 181.
(8) Kajiyama, T.; Morotomi, N.; Hiraoka, S.; Takahara, A. *Chem. Lett.* **1987**, 1737.
(9) Kunitake, T.; Tawaki, S.; Nakashima, N. *Bull. Chem. Soc. Jpn.* **1986**, *53*, 3935.
(10) Kunitake, T.; Okahata, Y.; Yasunami, S. *J. Am. Chem. Soc.* **1982**, *104*, 5547.
(11) Kajiyama, T.; Kumano, A.; Takayanagi, M.; Okahata, Y.; Kunitake, T. *Chem. Lett.* **1984**, 915.
(12) Kumano, A.; Kajiyama, T.; Takayanagi, M.; Okahata, Y.; Kunitake, T. *Ber. Bunsen-Ges. Phys. Chem.* **1984**, *88*, 1216.
(13) Kumano, A.; Kajiyama, T.; Takayanagi, M.; Okahata, Y.; Kunitake, T. *Bull. Chem. Soc. Jpn.* **1985**, *58*, 1205.
(14) Kunitake, T.; Higashi, N.; Kajiyama, T. *Chem. Lett.* **1984**, 717.
(15) Higashi, N.; Kunitake, T. *Chem. Lett.* **1986**, 105.
(16) Higashi, N.; Kunitake, T.; Kajiyama, T. *Macromolecules* **1986**, *19*, 1362.
(17) Takahara, A.; Higashi, N.; Kunitake, T.; Kajiyama, T. *Macromolecules* **1988**, *21*, 2443.
(18) Nakagawa, T.; Ohyanagi, Y. In *Recent Developments in Statistical Inference and Data Analysis*; Matsushita, K., Ed.; North-Holand: Amsterdam, 1980.
(19) Luzatti, V.; Husson, F. *J. Cell Biol.* **1962**, *12*, 207.
(20) Hoffman, S. In *Practical Surface Analysis*; Briggs, D., Seah, M. P., Eds.; Wiley: New York, 1983.
(21) Wheeler, D. R.; Peppas, S. V. *Surf. Interface Anal.* **1987**, *10*, 153.
(22) Hazell, L. B.; Brown, I. S.; Freisinger, F. *Surf. Interface Anal.* **1986**, *8*, 25.
(23) Ashley, J. C. *IEEE Trans. Nucl. Sci.* **1980**, *NS-27*, 1454.
(24) Ashley, J. C.; Williams, M. W. *Radiat. Res.* **1980**, *81*, 364.
(25) Andrade, J. D. In *Surface and Interfacial Aspects in Biomedical Polymers*; Andrade, J. D., Ed.; Plenum: New York, 1986; Vol. 1, pp 184–186.